Lagrangian Transport Calculations Using *UARS* Data. Part II: Ozone

G. L. MANNEY,* R. W. ZUREK,* L. FROIDEVAUX,* J. W. WATERS,* A. O'NEILL,** AND R. SWINBANK@

*Jet Propulsion Laboratory/California Institute of Technology, Pasadena, California

**Centre for Global Atmospheric Modelling, Reading, United Kingdom

@Meteorological Office, Bracknell, United Kingdom

(Manuscript received 14 March 1994, in final form 14 February 1995)

ABSTRACT

Trajectory calculations are used to examine ozone transport in the polar winter stratosphere during periods of the *Upper Atmosphere Research Satellite* (*UARS*) observations. The value of these calculations for determining mass transport was demonstrated previously using *UARS* observations of long-lived tracers. In the middle stratosphere, the overall ozone behavior observed by the Microwave Limb Sounder in the polar vortex is reproduced by this purely dynamical model. Calculations show the evolution of ozone in the lower stratosphere during early winter to be dominated by dynamics in December 1992 in the Arctic. Calculations for June 1992 in the Antarctic show evidence of chemical ozone destruction and indicate that ≈50% of the chemical destruction may be masked by dynamical effects, mainly diabatic descent, which bring higher ozone into the lower-stratospheric vortex. Estimating differences between calculated and observed fields suggests that dynamical changes masked ≈20%–35% of chemical ozone loss during late February and early March 1993 in the Arctic. In the Antarctic late winter, in late August and early September 1992, below ≈520 K, the evolution of vortex-averaged ozone is entirely dominated by chemical effects; above this level, however, chemical ozone depletion can be partially or completely masked by dynamical effects. Our calculations for 1992 showed that chemical loss was nearly completely compensated by increases due to diabatic descent at 655 K.

1. Introduction

An important and complex problem in understanding the distribution and evolution of ozone in the stratosphere is that of distinguishing chemical from dynamical effects. This is particularly true in the Arctic during Northern Hemisphere (NH) winter, as the strong wave activity there produces a significant poleward and downward transport of lower-latitude ozone, as well as a generally warmer polar stratosphere when compared to the Southern Hemisphere (SH). The latter limits the extent and duration of regions of activated chlorine and the associated chemical loss of ozone, while the former enhances the contribution of transport in the seasonal evolution of ozone in the wintertime Arctic. Even so, Manney et al. (1994a) were able to show that the decrease in ozone in the Arctic lower stratosphere during late winter 1993, as observed by the Microwave Limb Sounder (MLS) onboard the *Upper Atmosphere Research Satellite* (*UARS*), was inconsistent with transport inferred from the evolution of the long-lived stratospheric tracers nitrous oxide (N_2O) and methane (CH_4), as observed simultaneously by the Cryogenic Limb Array Etalon Spectrometer (CLAES). This observed ozone decrease, which was the largest seen in the northern polar vortex during the winters observed there by *UARS* instruments, was consistent with estimates of chemical loss based on observations by MLS of the key catalytic chemical radical, chlorine monoxide (ClO). However, the uncertainties associated with the calculation of chemical loss were large in the absence of detailed knowledge of the history of air motions (e.g., exposure to sunlight), and it was uncertain to what extent transport of ozone had masked the true amount of chemical depletion.

One approach that can be used where observations of ozone and meteorological fields are available is to model ozone transport using winds derived from observations but ignoring chemical processes. Differencing the fields thus modeled with observed fields then provides an estimate of the nonconservative chemical processes. This residual also contains, of course, the effects of inaccuracies in the model calculations and the wind fields used in those calculations and the effects of observational errors in the ozone distribution itself.

Corresponding author address: Dr. Gloria Manney, Jet Propulsion Laboratory, Mail Stop 183-701, 4800 Oak Grove Dr., Pasadena, CA 91109-8099.

by also simulating the distributions of the passive tracers N_2O and CH_4. Furthermore, by focusing on the large-scale patterns the effect of random errors can be reduced.

Manney et al. (1995a, hereafter Part I) studied the transport of the passive tracers observed by CLAES and of water vapor observed by MLS. Transport of these tracers was computed by filling the model stratosphere with air parcels and computing their trajectories for approximately one month. Trace gas concentrations were computed from these trajectories by assigning to each parcel the observed value of the tracer mixing ratio on the initial day. Concentrations at later times are determined by the three-dimensional advection of parcels containing these initial values. The evolving fields, determined by trajectories computed using horizontal winds from the U.K. Meteorological Office (UKMO) data assimilation system (interpolated to isentropic surfaces) and vertical (cross isentropic) winds computed with a radiative transfer code, can then be compared with observations either by gridding the tracer concentrations of parcels near a given grid point or by interpolating the observations to the advected parcel locations. Some advantages and disadvantages of this approach are discussed in Part I.

The four time periods listed in Table 1 are examined here. These periods are the times when both MLS and CLAES could observe the middle and high latitudes of the winter hemisphere during both early and late winter periods. (Because of the precessing, 57° inclined orbit of UARS and their limb-viewing directions being orthogonal to one side of the spacecraft track, MLS and CLAES view middle and high latitudes of alternate hemispheres approximately every 36 days.) This permits a contrast between the NH and SH, as well as between early and late winter, periods when different amounts of reactive chlorine were present and when planetary wave activity also differs. Waters et al. (1993a,b) show that, during the two SH time periods mentioned above, elevated values of ClO were present in most of the sunlit portion of the polar vortex in the lower stratosphere. Slightly enhanced ClO was observed at some times in the NH in December 1992 (Manney et al. 1994a; Waters et al. 1995). In February 1993, enhanced ClO values in the NH were comparable to those in the SH in August 1992 (Waters et al. 1993a) but decreased during that observing period (Manney et al. 1994a).

In Part I, the transport of passive tracers observed by CLAES and MLS was studied for the same periods. Since the trajectory scheme successfully reproduced the large-scale distributions of N_2O and CH_4 in middle and high latitudes, we have some confidence that it would reproduce the general features of the observed extratropical ozone distribution in the middle and lower stratosphere, if ozone were nearly conserved over the 20–30-day time periods considered here. Thus, differences between the calculated and observed ozone fields are indicative of chemical loss. In this way, we place some limits on how much of the observed ozone evolution can be explained solely by transport processes and thus establish the potential extent to which transport may mask chemical loss during these periods.

2. Data and analysis

The trajectory calculations are described in Part I and in Manney et al. (1994b). Horizontal winds are from the UKMO data assimilation system (Swinbank and O'Neill 1994) and vertical velocities from a recent version of the middle atmosphere radiation code MIDRAD, an earlier version of which is described by Shine (1987). Temperatures used in the radiation code are from the UKMO data; the radiation code uses MLS ozone, except for the June 1992 run when continuous reliable ozone data were not available. Manney et al. (1994b) discuss some limitations of the radiation calculation and differences seen between heating rates calculated using climatological and MLS ozone. The trajectory code (Manney et al. 1994b) uses a standard fourth-order Runge–Kutta scheme. Winds and temperatures are interpolated linearly in time from the once daily values to the trajectory time step ($1/2$ h). Heating rates are recalculated every 3 h using interpolated temperatures and are interpolated linearly to the trajectory time step between calculations. Further details of the trajectory calculation are given by Manney et al. (1994b) and of the initialization of parcels in Part I.

The Rossby–Ertel potential vorticity (PV) is also calculated from the UKMO data (Manney and Zurek 1993) and is compared with calculated and observed tracer fields. When examining vertical cross sections, PV is scaled in "vorticity units" using a standard atmosphere value of the static stability (Dunkerton and Delisi 1986; Manney et al. 1994b); this gives a similar range of values for PV on isentropic surfaces throughout the stratosphere.

TABLE 1. Periods examined using trajectory calculations.

Period	NH or SH viewing	ClO enhancement	Wave activity
3 Dec 1992–2 Jan 1993	NH	Little	Active
14 Feb 1993–16 Mar 1993	NH	Large, but decreasing	Active, large events
15 Jun 1992–5 Jul 1992	SH	Some	Little activity
19 Aug 1992–18 Sep 1992	SH	Large and persistent	Some activity

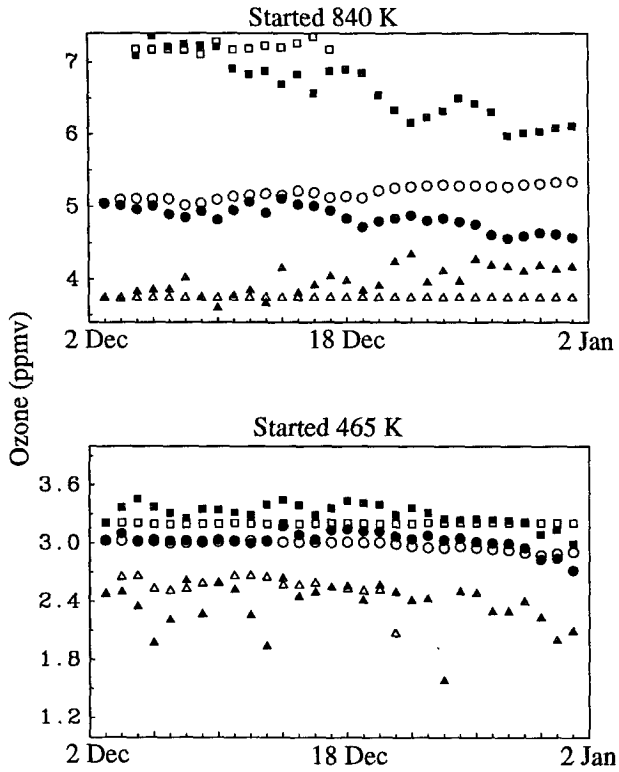

FIG. 1. The average (circles), minimum (triangles), and maximum (squares) values of ozone mixing ratios (ppmv) as computed by interpolating gridded MLS observations to the parcel locations determined by trajectory calculations (solid symbols) and as computed directly from the conserved initial ozone mixing ratios associated with these parcels (open symbols) for 3 Dec 1992–1 Jan 93. The ensemble of air parcels used was initialized at 840 K (a) or 465 K (b) and is constrained to have a scaled PV > 1.4×10^{-4} s^{-1} on the day considered.

The ozone data are from the MLS 205-GHz radiometer; they have a horizontal resolution of ≈400 km and an intrinsic vertical resolution of ≈4 km, although current retrievals are done at ≈5.5-km spacing. The *UARS* MLS instrument is described by Barath et al. (1993), and retrieval methods are summarized by Froidevaux et al. (1994). Precisions (rms) of individual ozone measurements for the altitudes examined here are ≈0.3 ppmv, with absolute accuracies of ≈5%–15% (Froidevaux et al. 1994). Ozone data are gridded using Fourier transform techniques that separate time and longitude variations (Elson and Froidevaux 1993).

Air parcels are initialized on the grid described in Part I, on 15 June 1992 and 19 August 1992 in the SH, and 3 December 1992 and 14 February 1993 in the NH; the trajectory code was run for 20 days for the June 1992 case and 30 days for each of the other cases. The general motions of air parcels during these time periods were described by Manney et al. (1994b). The method used to grid the calculated fields from values at the advected parcel positions is described in Part I, along with possible biases that may be introduced by the gridding procedure. The types of analyses used to compare calculated and observed fields are also discussed in detail in Part I.

Ozone is mostly produced in the midstratosphere at low latitudes (e.g., Brasseur and Solomon 1984). The purely advective calculation described in Part I will not maintain that source over the time period of the runs considered here; test calculations for February and March 1993 showed that the calculated fields diverged from the observed fields during the 30-day runs at altitudes above ≈1000 K and equatorward of ≈25° above ≈600 K because there was no mechanism for maintaining high ozone mixing ratios at the equator. To alleviate this problem, while still maintaining dynamically controlled fields in the middle and lower stratosphere at middle and high latitudes, we parameterize standard gas phase ozone photochemistry by relaxing the ozone field to values observed by MLS each day during the gridding procedure. The relaxation time constant is dependent on latitude, altitude, and day of year, and is based on Fig. 11 of Garcia and Solomon (1985). Below ≈30 km, and in high-latitude regions for all altitudes considered here, relaxation time constants are much longer than the 30 days for which these runs are done. At ≈32 km (near 840 K, the highest level examined in detail here) at 40° latitude, the final field on a given day contains ≈95% of the field calculated for that day and 5% of the observed field, with the contribution of the observed field dropping off rapidly with increasing latitude and decreasing altitude. The net effect of this procedure is to force parcels in

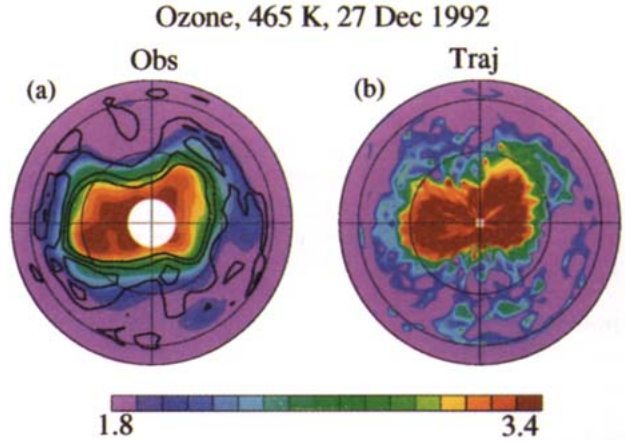

FIG. 2. Synoptic maps of ozone at 465 K from observations and trajectory calculations on day 24 (27 Dec 1992) of NH early winter run. The projection is orthographic, with 0° longitude at the bottom of the plot and 90°E to the right; dashed lines show 30° and 60° latitude circles; PV contours in the region of strong PV gradients are overlaid on the plots of observed values; these contours are 0.2, 0.25, and 0.3×10^{-4} K $m^2 kg^{-1}$ s^{-1}.

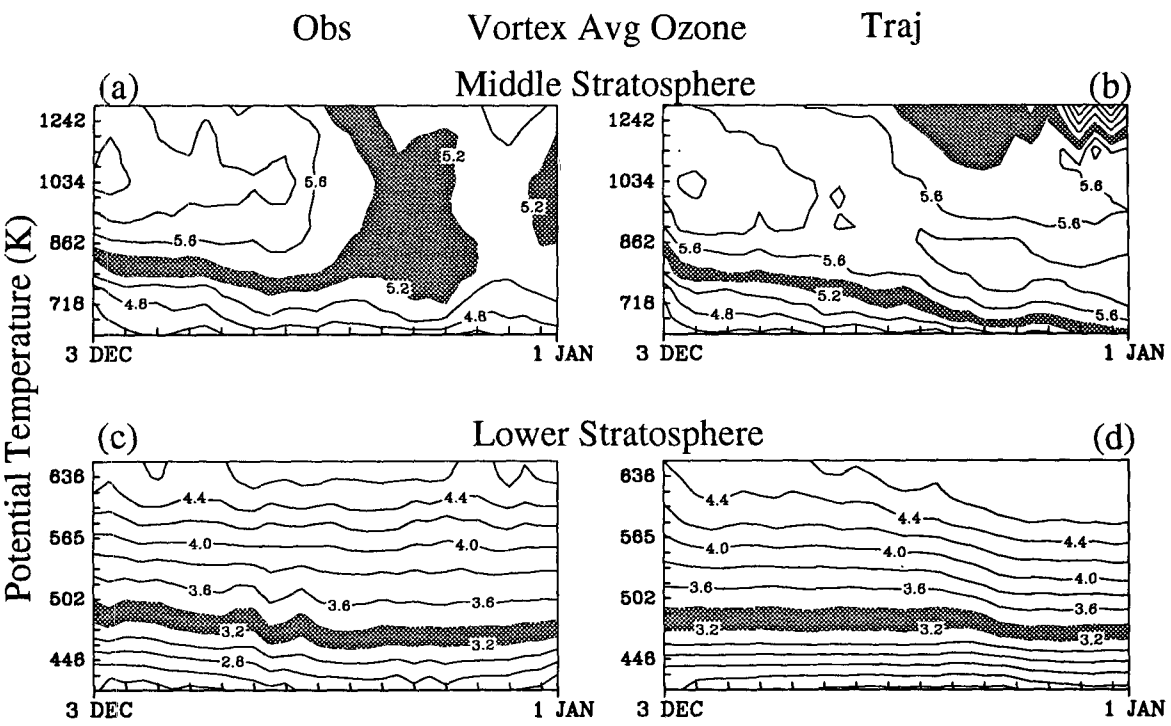

FIG. 3. Time series for 3 Dec 1992–1 Jan 1993 of vortex-averaged ozone mixing ratios (ppmv) as a function of θ in the middle stratosphere (655–1300 K) (a and b) and lower stratosphere (420–655 K) (c and d) from observations (a and c) and gridded calculations (b and d). Vortex averages are area weighted and are computed using the 1.4×10^{-4} s^{-1} scaled PV contour as an approximate definition of the vortex edge. Values between 5.2 and 5.4 ppmv are shaded in (a) and (b), and values between 3.2 and 3.4 ppmv in (c) and (d).

low latitudes in the middle and upper stratosphere on a given day to high ozone values. The procedure, with the time constants used here, results in holding ozone close to its observed values at latitudes equatorward of ≈20°–30° at altitudes above ≈28 km and at most latitudes above ≈40 km, and allowing advection to determine its distribution elsewhere. Tests done using this procedure and the purely advective one show differences above ≈800 K after about the first 10 days of the runs; no discernable differences are seen below ≈650 K. This is acceptable for this study, which focuses on middle and high latitudes in the middle and lower stratosphere.

Gridded fields were also obtained using the reverse trajectory procedure described in Part I, similar to that used by Sutton et al. (1994). Since application of the relaxation in that procedure would not be feasible due to its additional computational demands, these are done without the relaxation; the results are thus comparable to the results of the other procedure only at levels below ≈650–700 K. These results for the lower stratosphere have been compared to those using the binning and interpolation gridding procedure to assess the sensitivity to the gridding and will be discussed at appropriate points in the text.

3. Results

a. Early winter

1) NORTHERN HEMISPHERE, 3 DECEMBER 1992–2 JANUARY 1993

Figure 1 shows time series of the average, minimum, and maximum observed ozone mixing ratios interpolated to parcel positions for parcels initialized at 840 and 465 K and with scaled PV $\geq 1.4 \times 10^{-4}$ s^{-1} (i.e., inside the polar vortex). The open symbols show the values predicted by the trajectory calculations each day; these would not change except that, as described in Part I, the number of parcels in this region varies from day to day. For the parcels initialized at 465 K, no significant trend is seen between the observed and calculated average ozone mixing ratios, indicating that dynamics is the main factor in the evolution of these fields and that the trajectory calculations do a reasonable job of reproducing the average characteristics. Note that more fluctuation and greater differences are expected in the minimum and maximum values, as these depend upon single parcel locations within the vortex, while the vortex-averaged values are typically summed over 800 parcels or more. This averaging re-

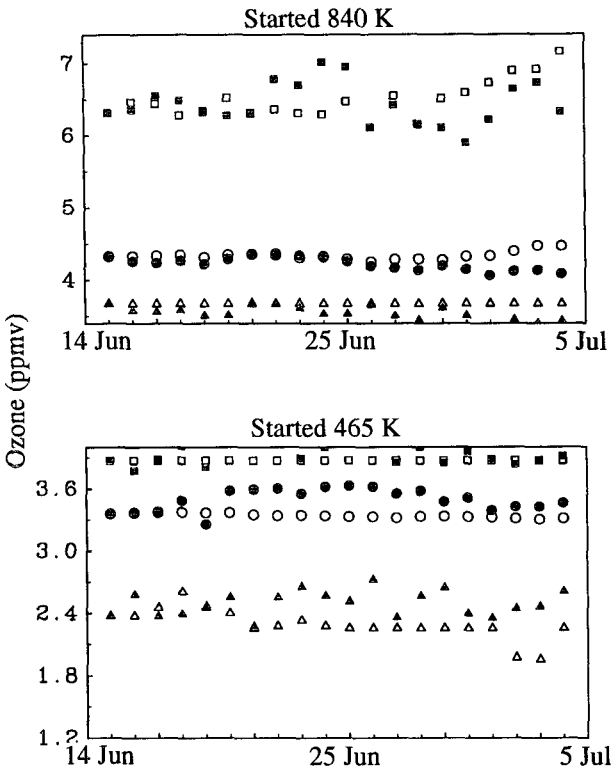

FIG. 4. As in Fig. 1 but for 15 Jun–4 Jul 1992 in the SH; |PV| greater than 1.4×10^{-4} s^{-1} is used in the SH.

duces both measurement error and spatial bias due to lack of coverage.

At 840 K, the trajectory calculations yield a small increase in the maximum and average values, suggesting parcels with higher ozone have moved into the vortex in the middle stratosphere. By contrast, ozone observed at the parcel locations steadily decreases. In Part I, the passive tracers studied suggested that the computed diabatic descent was on average too strong in the polar middle and upper stratosphere during the latter part of this early winter period. Since ozone increases with height in the Arctic vortex middle stratosphere, most of the decrease in vortex-averaged ozone shown in Fig. 1a is consistent with this overestimate of descent, and it is not necessary to invoke nonconservative processes.

Figure 2 shows synoptic maps of observed and calculated ozone at 465 K on day 24 (27 December 1992) of this run. Good agreement is seen between these observed and calculated fields. The calculated field shows high ozone over a somewhat larger portion of the vortex and stronger gradients along the vortex edge. As noted in Part I, the calculations contain no parameterization of small-scale mixing, which would tend to reduce the gradients; also, the low horizontal resolution of the MLS measurements may yield unrealistically weak gradients. Synoptic maps in the midstratosphere (not shown) indicate, as was the case for the passive tracers studied in Part I, that anticyclonic features in midlatitudes are washed out by the end of this run.

Figure 3 shows vortex-averaged observed and calculated ozone in the lower (465–655 K) and middle (655–1300 K) stratosphere. These show reasonable agreement throughout the period below ≈550 K, although the observed ozone increase appears to occur earlier and more gradually. Above ≈550 K, Fig. 3 shows greater downward motion of the contours in the calculations than in the observations. The decrease in observed vortex-averaged ozone in the middle of the period and slight increase at the end of the period are also apparent in the calculations but are not nearly as pronounced. The rapid increase at 1300 K in the last few days of the calculation is due to that level becoming devoid of parcels near the pole, where the lowest ozone values would be. Differences above ≈900 K may also be influenced by the overly simplistic parameterization of ozone photochemistry. Difference plots over the period similar to those presented in Part I (not shown) indicate the same general patterns of decrease in observations and calculations but show much larger increases at high PV values in calculations than in observations, which is consistent with calculated diabatic descent being too strong there. The results shown here for ozone are consistent with those shown in Part I for passive tracers.

2) SOUTHERN HEMISPHERE, 15 JUNE–5 JULY 1992

Figure 4 shows time series, for 15 June–5 July 1992 in the SH at 840 and 465 K, of the average, minimum, and maximum observed ozone mixing ratios interpolated to parcel positions for parcels with scaled |PV| $\geq 1.4 \times 10^{-4}$ s^{-1} in the polar vortex, as was shown in Fig. 1 for the NH. At 465 K, there is little trend of observations with respect to calculations. At 840 K, the observations decrease slightly with respect to the calculations in the last few days of the run. The differences in both cases are small, suggesting that at the levels shown the evolution of ozone is governed mainly by dynamics.

Figure 5 shows vortex-averaged ozone in the lower and middle stratosphere for this period. In the middle stratosphere, observations and calculations show the same general patterns for the first ≈15 days of the run, after which the calculated fields show greater downward motion of the contours. In the lower stratosphere, while both observed and calculated contours are relatively flat at the lowest levels, at ≈500–600 K the observations show a decrease in ozone while calculations show a slight increase. The behavior seen in the observations is also inconsistent with the behavior of passive tracers shown in Part I. At ≈550 K, if changes in the ozone field were caused by vertical motion, the ob-

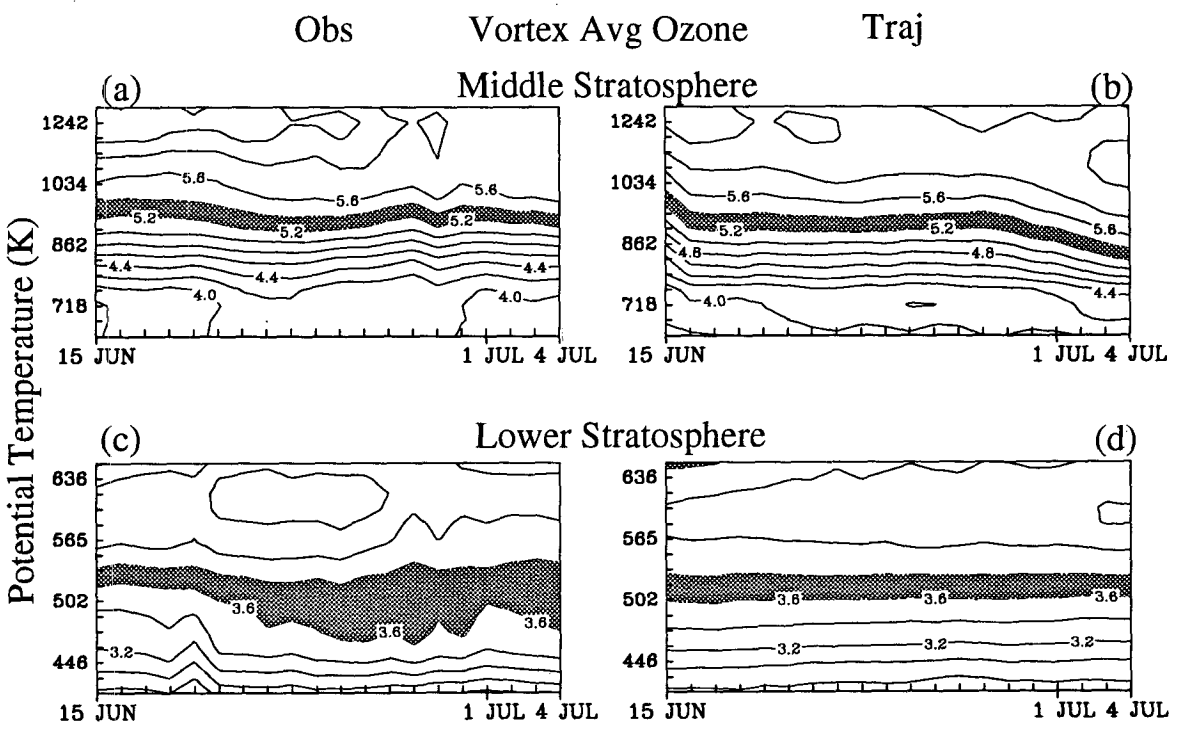

FIG. 5. As in Fig. 3 but for 15 Jun–4 Jul 1992 in the SH; |PV| greater than 1.4 × 1-$^{-4}$ s^{-1} is used in the SH. Values between 3.6 and 3.8 ppmv are shaded in (c) and (d).

served evolution would imply a vortex-averaged diabatic *ascent* of ≈1.5 K/d near that level. Since Manney et al. (1994b) and Part I conclude that there is in fact significant diabatic *descent* during this period (between ≈−0.7 and ≈−1.2 K/d), and since Manney et al. (1994b) show that there is little mixing across the PV contour used here to define the vortex average, it is unlikely that the observed changes in ozone between 500 and 600 K during June 1992 could be caused by dynamics alone. Waters et al. (1993b) showed significant enhancement of ClO in sunlit regions at 22 hPa (near 600 K) at this time; thus, chemical loss would be expected.

Figure 6 shows an estimate of the nondynamical vortex-averaged change in ozone (presumed to be chemical destruction) after the initial day of the run. The observed and calculated changes in ozone are plotted; we assume that the calculated change represents all dynamical changes (presumably mainly due to diabatic descent in this case), and thus the change that would be seen if dynamics were removed is obtained by subtracting that change from the observed change. This figure indicates that there may have been chemical ozone loss at this level over this period of ≈0.25 ppmv and that ≈1/2 of this loss was masked by dynamical processes. The nondynamical change represents a decrease of ≈0.3%/d, if taken over the entire 20-day period, or ≈0.6%/d over the last half of the period. The passive tracer study (Part I) suggested that the trajectory calculations may underestimate diabatic descent in the SH lower stratosphere during this period; if so, the actual chemical loss would be correspondingly larger.

b. Late winter

1) NORTHERN HEMISPHERE, 14 FEBRUARY – 16 MARCH 1993

Figure 7 shows time series for 14 February–15 March 1993 of the average, minimum, and maximum

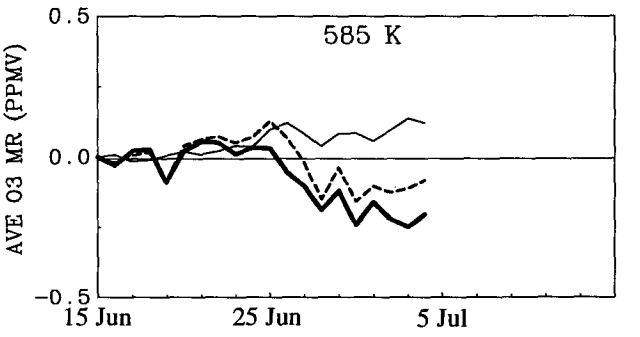

FIG. 6. Observed (heavy dashed line) and calculated (thin dashed line) vortex-averaged (PV ≥ 1.4 × 10^{-4} s^{-1}) ozone change at 585 K and estimated nondynamical change (heavy solid line) for 15 Jun–4 Jul 1992 in the SH.

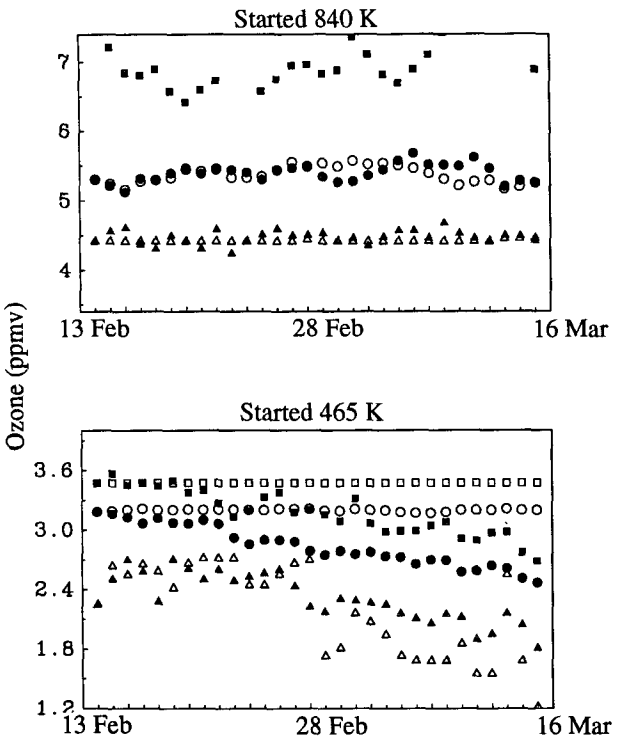

FIG. 7. As in Fig. 1 but for 14 Feb–15 Mar 1993.

observed ozone mixing ratios interpolated to parcel positions for parcels with scaled PV $\geq 1.4 \times 10^{-4}$ s^{-1} and initialized at 840 and 465 K in the NH polar vortex. At 840 K, there is little trend of observations with respect to calculations, although the observations temporarily diverge slightly from the calculations at the time of a strong stratospheric warming in early March (Manney et al. 1994c). The general agreement suggests that the changes are governed by dynamics.

Figure 8 shows synoptic maps from the gridded calculated fields compared with observations at 840 K on days 8 (22 February 1993) and 16 (2 March 1993). As was the case in Part I with the passive tracer fields, the transport calculation does a good job of reproducing the extent and shape of the region of low ozone in the polar vortex. The tongue of high ozone that is being drawn up around the edge of the vortex on 22 February is also apparent in the calculations but is somewhat larger than in observations. On 2 March, while the calculations show a region of high ozone in the anticyclone consistent with what was seen in Part I for passive tracers, the observations show relatively low ozone in that region. Manney et al. (1995b) have studied this phenomenon in detail and concluded that the behavior of ozone in a strong anticyclone at this level is inconsistent with what could be caused solely by transport.

At 465 K, Fig. 7 shows a steady decrease in the observations with respect to the calculations throughout the period. Previously, Manney et al. (1994a) showed that the decrease observed during this period was consistent with chemical ozone depletion and not with transport alone. Figure 9 shows synoptic maps of ozone at 465 K on days 20 (6 March 1993) and 30 (16 March 1993). The contrast between the amount of ozone calculated and observed in the vortex is dramatic, although the shape and position of the region of high ozone in each agrees very well.

Figure 10 shows vortex-averaged ozone in the lower and middle stratosphere for the period. The general features of the evolution in the middle stratosphere agree fairly well between observations and calculations, with similar increases in observed and calculated averages at the times of strong stratospheric warmings; as for the NH early winter warmings, these increases are somewhat smaller in the calculations. The downward movement of the contours is also similar in calculations and observations, suggesting reasonable agreement of diabatic descent rates.

In the lower stratosphere, the calculations show the contours moving gradually but steadily downward with time, while the observations show the opposite behavior. Figure 11 compares observed with calculated

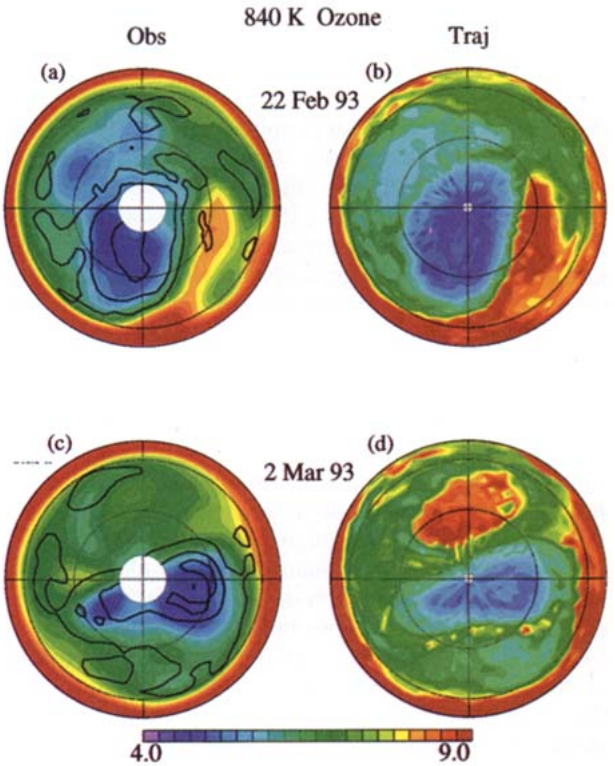

FIG. 8. Synoptic maps of ozone at 840 K from observations and trajectory calculations on days 8 (22 Feb 1993) and 16 (2 Mar 1993) of NH late winter run. Layout is as in Fig. 2; PV contours overlaid on observed plots are 3, 5, and 7 ($\times 10^{-4}$ K m^2 kg^{-1} s^{-1}).

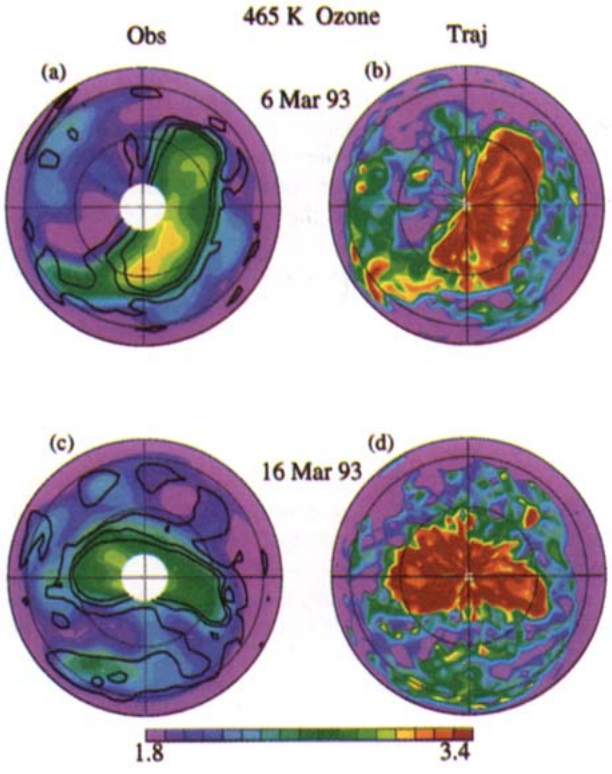

FIG. 9. As in Fig. 2 but for days 20 (6 Mar 1993) and 30 (16 Mar 1993) of NH late winter run.

changes in the lower stratosphere (420–840 K) between the end (16 March 1993) and beginning (14 February 1993) of the run. Figure 11a is similar to one shown by Manney et al. (1994a) but shows smaller changes because it is over a shorter time period and that time period excludes the first few days of late winter NH observations, when the steepest drop in lower stratospheric ozone and the highest amounts of ClO were observed by MLS. (The period shown here was dictated by showing the same period for which CLAES observations of N_2O and CH_4 were studied in Part I.) The observed and calculated plots in Fig. 11 show reasonable agreement above about ≈650 K, but, as expected, observed ozone decreases below that level over this period in the entire region inside the vortex (PV $\geq \approx 1.2 \times 10^{-4}$ s^{-1}). Meanwhile, calculations show slight increases over much of that region, with no decrease comparable to those in the observations.

Figure 12 shows plots similar to Fig. 7 for this period at 465, 520, and 585 K. The overall decrease seen in the observed fields at 465 K is again less than that shown by Manney et al. (1994a), because as noted earlier the first few days of observations, with their particularly steep decrease, are not included. Included in these plots are lines showing the calculated ozone changes and inferred chemical changes using the reverse trajectory procedure to obtain gridded fields. At 465 and 520 K, the reverse trajectory procedure suggests slightly more descent, and thus a slightly larger inferred chemical ozone loss, during the last ≈10 days of the period studied. This case shows the largest differences between the two gridding procedures of those studied here. The calculations shown in Fig. 12 suggest that dynamical effects are masking ≈20%–35% of the chemical loss at each level. The calculated vortex-averaged nondynamical (chemical) ozone decreases over the period shown are ≈0.45–0.5 ppmv at each level. This is ≈0.5%/d at 465 K and ≈0.4%/d at 585 K in the vortex average. Larsen et al. (1994) gave values for ozone changes for January–March 1993, corrected for diabatic descent, at stations in Greenland, of −1.1%/d at 475 K and −0.4%/d at 550 K. Since our calculations are vortex averaged, and over only the late part of their time period, they do not appear inconsistent with those of Larsen et al. (1994).

2) SOUTHERN HEMISPHERE, 19 AUGUST–18 SEPTEMBER 1992

Figure 13 shows time series for 19 August–17 September 1992 in the SH of the average, minimum, and maximum observed ozone mixing ratios interpolated to parcel positions for parcels initialized at 840 and 465 K and with scaled $|PV| \geq 1.4 \times 10^{-4}$ s^{-1} in the polar vortex. At 840 K, observations and calculations agree well until the last few days of the run, when calculations increase with respect to observations; this confirms that the evolution of ozone in the vortex at 840 K is dominated by transport. The fact that observations decrease with respect to calculations suggests that diabatic descent could be slightly too strong near this level; Part I gave little information about diabatic descent rates in the midstratosphere for this period because the gradients of N_2O and CH_4 were so weak in this region. At 465 K, observations decrease rapidly with respect to calculations, showing the widespread chemical ozone destruction occurring at this time.

Figure 14 shows synoptic maps of observed and calculated ozone at 840 K on day 16 (4 September 1992) of the run. As in the February–March 93 NH case, the model reproduces the extent and shape of the region of low ozone in the vortex and a tongue of high ozone drawn up from low latitudes. Again, as in the NH example, calculated ozone mixing ratios in the tongue are somewhat higher than observed values. Vortex averages in the middle stratosphere (not shown) show good agreement, with observed increases in the average during stratospheric minor warmings in early September (Manney et al. 1993) being reproduced in the calculations, and similar amounts of descent of the contours are seen in both calculations and observations.

Figure 15 shows maps of observed and calculated ozone on day 24 (12 September 1992) at 465 K, with

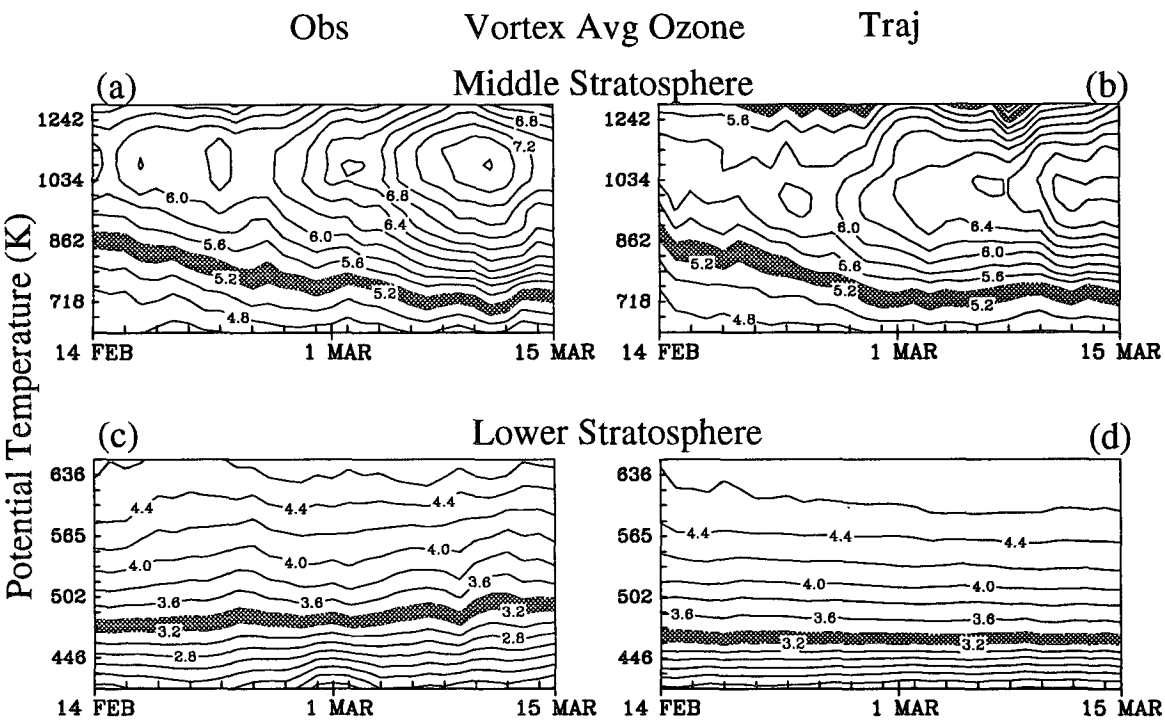

FIG. 10. As in Fig. 3 but for 14 Feb–15 March 1993.

the observations showing a well-developed ozone hole signature. Although the shape of the vortex region is comparable, the low values in observed compared to calculated fields show the unmistakably large chemical loss that has taken place.

Figure 16 shows difference plots in PV–θ space in the lower stratosphere (420–840 K) for both observations and calculations between the end (18 September 1992) and the beginning of the run (19 August 1992). Over the region of the polar vortex ($PV \leq \approx -1.2 \times 10^{-4}$ s^{-1}), and over nearly the entire vertical range of the plot, the observations show large decreases in ozone, whereas the calculations range from large increases in the upper levels to little or no change in the lowest levels. Vortex averages in the lower stratosphere (not shown) are consistent with this picture, with observed ozone decreasing rapidly in the lowest levels in observations, and some decreases noticeable up to 655 K (Manney et al. 1993; Manney et al. 1995c), and in the calculations, ozone increases above ≈500 K and little or no apparent change below ≈500 K. The lower stratospheric vortex-averaged ozone at the beginning of this period is already significantly lower than at the end of the early winter SH period shown in Fig. 5 (Manney et al. 1995c).

Figure 17 shows estimates of the nondynamical changes (similar to those shown in Figs. 6 and 12) at 520, 585, and 655 K. Using the reverse trajectory procedure to obtain gridded files gave nearly identical results in this case. At and below 520 K, vortex-averaged diabatic descent rates are very small (Part I), and therefore the chemical depletion entirely dominates the observed field. A decrease in ozone of ≈1.5%/d is seen at 465 K (Manney et al. 1993) and ≈1.0%/d at 520 K. The nondynamical changes suggest that dynamical effects [mainly diabatic descent in this case, since the vortex is well confined; Manney et al. (1994b)] are masking ≈1/2 of the expected chemical decrease at 585 K and nearly all of it at 655 K. The implied chemical ozone loss is ≈0.5%/d at both 585 and 655 K. As noted in Part I, the radiation calculation used here may underestimate diabatic descent in some regions in the lower stratosphere, so chemical destruction could be even larger than these estimates.

4. Conclusions

Trajectory calculations are used to examine ozone changes in the polar winter stratosphere during periods of *UARS* observations. The value of these trajectory calculations for determining mass transport in the polar lower and middle stratosphere was demonstrated in Part I using passive tracer observations by CLAES. Comparisons with observations provide information on where and when the observed evolution of ozone can or cannot be explained solely by dynamical processes.

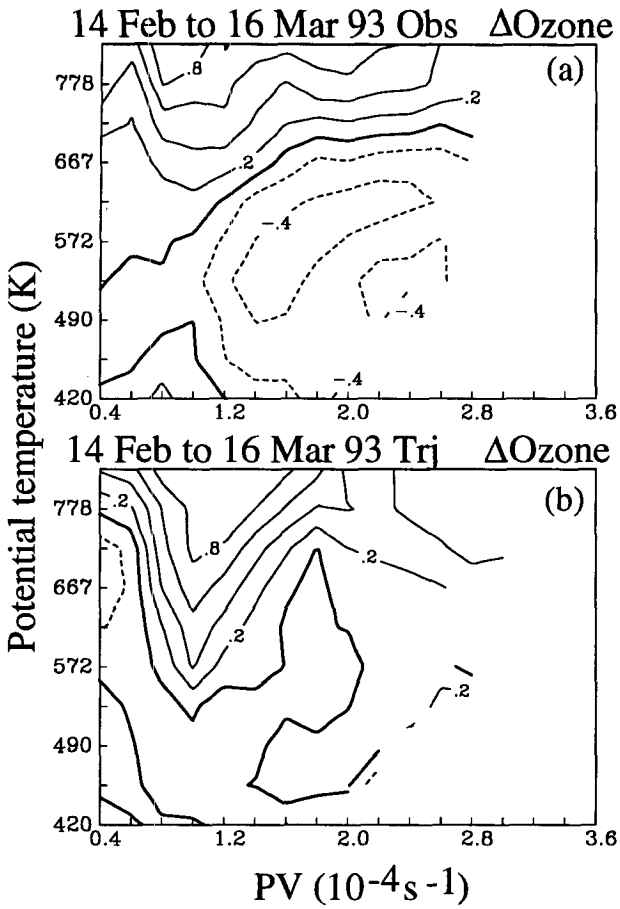

FIG. 11. Differences (ppmv) in (a) observed and (b) calculated ozone fields in the lower stratosphere (420–840 K) between 16 Mar 1993 and 14 Feb 1993, as a function of PV and θ; dashed lines indicate a decrease over the time period.

Four time periods are considered, covering early and late winter in the NH and the SH, when both *UARS* MLS ozone and CLAES passive tracer observations were available for high latitudes.

In the middle stratosphere, ozone in the polar vortex is shown to behave in a manner consistent with the behavior of passive tracers discussed in Part I during each of the periods discussed here. In both NH and SH late winter periods, the calculations also reproduce tongues of high ozone that are drawn up from low latitudes around the edge of the polar vortex. Calculations also show isolated regions of high ozone in the anticyclone during some of these events where observations show low values, indicating that ozone does not behave like a passive tracer here, as discussed in detail by Manney et al. (1995b). Although not emphasized here, vortex averages show temporary increases in ozone during stratospheric warmings in the calculations similar to those seen in observations (Manney et al. 1995c).

In the early winter NH lower stratosphere, during December 1992, the average observed behavior of ozone was consistent with the calculations and with that of the passive tracers shown in Part I, indicating that the evolution of ozone in the lower stratosphere during December 1992 was dominated by dynamics. In the SH early winter lower stratosphere, during late June and early July 1992, enhanced ClO was reported by Waters et al. (1993b). A decrease in vortex-averaged ozone

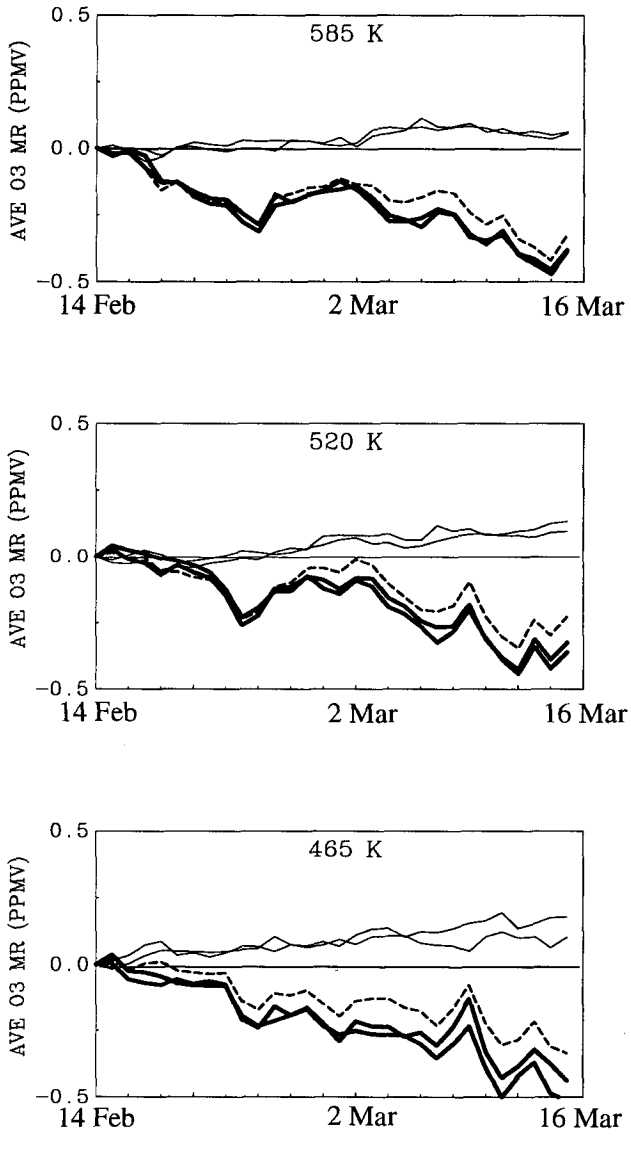

FIG. 12. As in Fig. 6 but for 14 Feb–15 March 1993 in the NH at 465, 520, and 585 K. The second thin and thick solid lines show the vortex-averaged calculated ozone and inferred chemical loss from the reverse trajectory gridding procedure, as described in the text; the reverse trajectory procedure gives higher values at the end of the period for calculated ozone at 465 and 520 K and therefore lower values for inferred chemical loss.

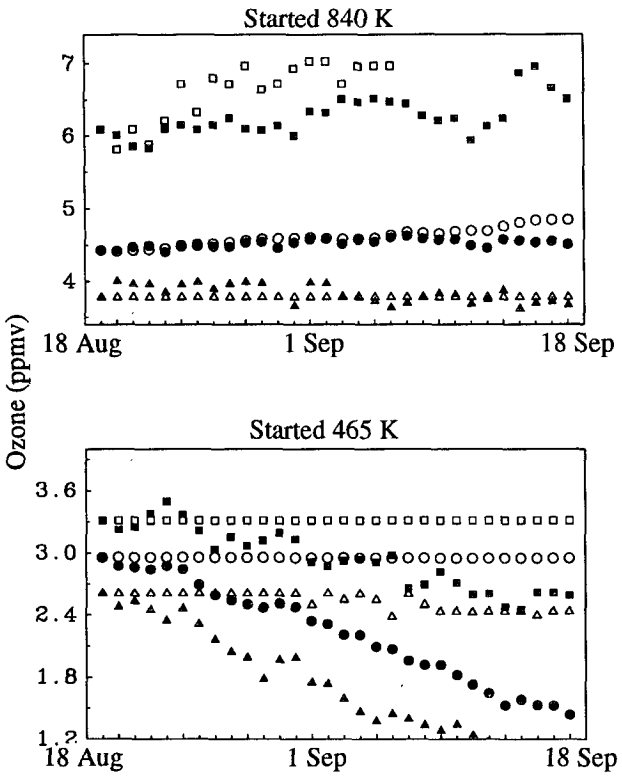

FIG. 13. As in Fig. 4 but for 19 Aug–17 September 1992.

of the passive tracers shown in Part I, indicating that the evolution of ozone in the lower stratosphere during December 1992 was dominated by dynamics. In the SH early winter lower stratosphere, during late June and early July 1992, enhanced ClO was reported by Waters et al. (1993b). A decrease in vortex-averaged ozone between ≈500 and 600 K is shown here during the

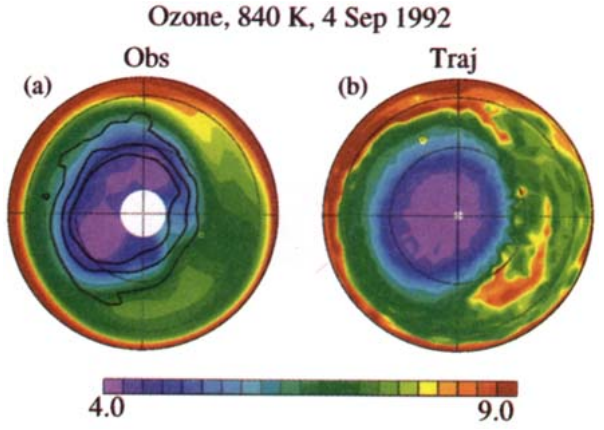

FIG. 14. As in Fig. 8 but for day 16 (4 Sep 1992) of SH late winter run; 0° longitude is at the top of the plot, and 90°E to the right; PV contours are −3, −5, and -7×10^{-4} K m^2 kg^{-1} s^{-1}.

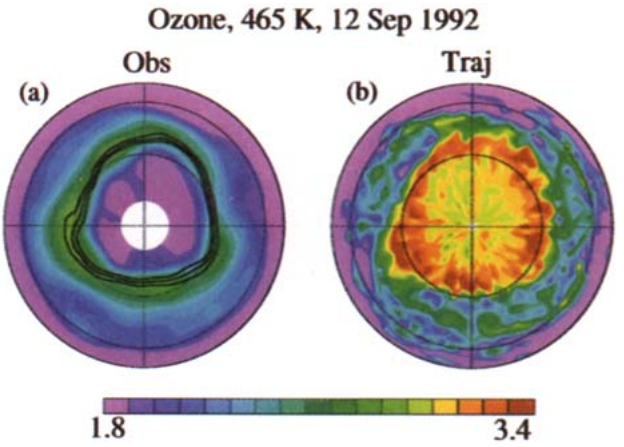

FIG. 15. As in Fig. 9 but for day 24 (12 Sep 1992) of SH late winter run; 0° longitude is at the top of the plot, and 90°E to the right; PV contours are −0.2, −0.25, and -0.3×10^{-4} K m^2 kg^{-1} s^{-1}.

latter half of the period, where calculations show ozone should be increasing due to significant diabatic descent. Estimates using the calculated fields to remove dynam-

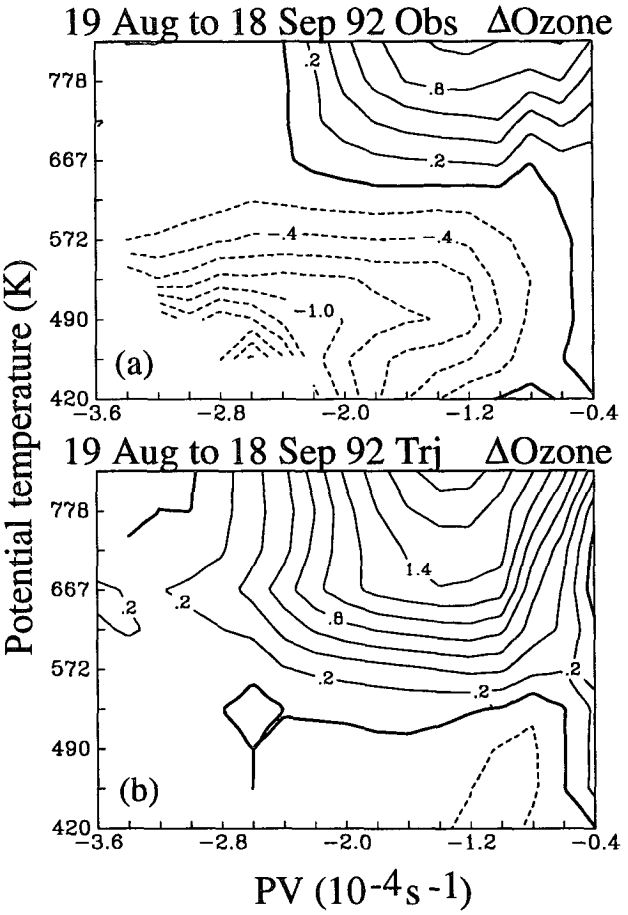

FIG. 16. As in Fig. 11 but between 18 Sep 1992 and 19 Aug 1992.

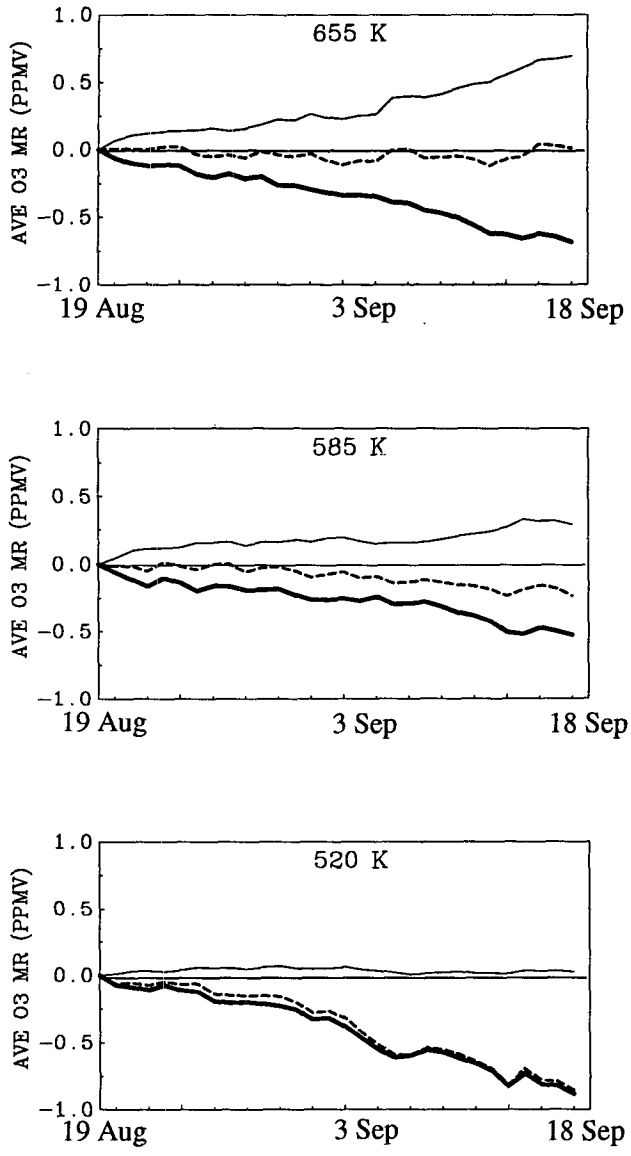

FIG. 17. As in Fig. 6 but for 19 Aug–17 Sep 1992 at 520, 585, and 655 K; $|PV| \geq 1.2 \times 10^{-4}$ s^{-1} is used for the average here.

et al. 1993) and during the February–March 1993 NH period (Manney et al. 1994a). Estimates using the differences between the calculated and observed fields suggest that dynamical effects in the NH during late February and early March 1993 mask ≈20%–35% of the vortex-averaged chemical ozone destruction at levels from 465 to 585 K. In the SH during late August and early September 1992, diabatic descent rates below ≈520 K are so small and chemical losses so large that ozone changes observed in the lower stratosphere are entirely dominated by chemical effects. At levels up through 655 K, however, transport can significantly mask chemical losses, with up to 50% of the vortex-averaged loss being masked at 585 K and potentially all of it at 655 K. This means that observed ozone variations are affected by dynamical processes in two important ways. First, they modulate the meteorological conditions necessary for the formation and isolation of reactive forms of chlorine. Second, the transport of ozone during the seasons when ozone will be chemically lost in the polar vortex due to reactions with chlorine compounds can mask the amount or spatial extent of chemical depletion of ozone. Both of these dynamical effects are themselves modulated by interannual variability in the stratosphere and potentially by longer-term climate changes.

Acknowledgments. We thanks our MLS colleagues for their continued collaboration and support: L. S. Elson for providing gridded MLS data, T. Luu for data management, P. A. Newman for routines that were adapted to calculate PV, J. L. Sabutis for a routine that was adapted to relax ozone to observed values, and M. L. Santee for helpful comments. This research was sponsored by NASA's Upper Atmosphere Research Satellite Project and was performed at the Jet Propulsion Laboratory/California Institute of Technology under contract with the National Aeronautics and Space Administration.

REFERENCES

Barath, F. T., and Coauthors, 1993: The Upper Atmosphere Research Satellite Microwave Limb Sounder instrument. *J. Geophys. Res.*, **98,** 10 751–10 762.

Brasseur, G., and S. Solomon, 1984: *Aeronomy of the Middle Atmosphere.* Reidel, 441 pp.

Dunkerton, T. J., and D. P. Delisi, 1986: Evolution of potential vorticity in the winter stratosphere of January–February, 1979. *J. Geophys. Res.*, **91,** 1199–1208.

Elson, L. S., and L. Froidevaux, 1993: The use of Fourier transforms for asynoptic mapping: Early results from the Upper Atmosphere Research Satellite Microwave Limb Sounder. *J. Geophys. Res.*, **98,** 23 039–23 049.

Froidevaux, L., J. W. Waters, W. G. Read, L. S. Elson, D. A. Flower, and R. F. Jarnot, 1994: Global ozone observations from *UARS* MLS: An overview of zonal mean results. *J. Atmos. Sci.*, **51,** 2846–2866.

Garcia, R. R., and S. Solomon, 1985: The effect of breaking gravity waves on the dynamics and chemical composition of the mesosphere and lower thermosphere. *J. Geophys. Res.*, **90,** 3850–3868.

Larsen, N., B. Knudsen, I. S. Mikkelsen, T. S. Jorgensen, and P. Eriksen, 1994: Ozone depletion in the Arctic stratosphere in early 1993. *Geophys. Res. Lett.*, **21,** 1611–1614.

Manney, G. L., and R. W. Zurek, 1993: Interhemispheric comparison of the development of the stratospheric polar vortex during fall: A 3-dimensional perspective for 1991–1992. *Geophys. Res. Lett.*, **20,** 1275–1278.

——, L. Froidevaux, J. W. Waters, L. S. Elson, E. F. Fishbein, R. W. Zurek, R. S. Harwood, and W. A. Lahoz, 1993: The evolution of ozone observed by UARS MLS in the 1992 late winter southern polar vortex. *Geophys. Res. Lett.*, **20,** 1279–1282.

——, and Coauthors, 1994a: Chemical depletion of ozone in the Arctic lower stratosphere during winter 1992–1993. *Nature,* **370,** 429–434.

evolution of ozone observed by UARS MLS in the 1992 late winter southern polar vortex. *Geophys. Res. Lett.*, **20,** 1279–1282.

——, and ——, 1994a: Chemical depletion of ozone in the Arctic lower stratosphere during winter 1992–1993. *Nature,* **370,** 429–434.

——, R. W. Zurek, A. O'Neill, and R. Swinbank, 1994b: On the motion of air through the stratospheric polar vortex. *J. Atmos. Sci.*, **51,** 2973–2994.

——, ——, ——, ——, J. B. Kumer, J. L. Mergenthaler, and A. E. Roche, 1994c: Stratospheric warmings during February and March 1993. *Geophys. Res. Lett.*, **21,** 813–816.

——, and Coauthors, 1995a: Lagrangian transport calculations using *UARS* data. Part I: Passive tracers. *J. Atmos. Sci.*, **52,** 3049–3068.

——, and Coauthors, 1995b: Formation of low ozone pockets in the middle stratospheric anticyclone during winter. *J. Geophys. Res.*, in press.

——, L. Froidevaux, J. W. Waters, and R. W. Zurek, 1995c: Evolution of Microwave Limb Sounder ozone and the polar vortex during winter. *J. Geophys. Res.*, **100,** 2953–2972.

Shine, K. P., 1987: The middle atmosphere in the absence of dynamic heat fluxes. *Quart. J. Roy. Meteor. Soc.*, **113,** 603–633.

Sutton, R. T., H. Maclean, R. Swinbank, A. O'Neill, and F. W. Taylor, 1994: High resolution stratospheric tracer fields estimated from satellite observations using Lagrangian trajectory calculations. *J. Atmos. Sci.*, **51,** 2995–3005.

Swinbank, R., and A. O'Neill, 1994: A stratosphere–troposphere data assimilation system. *Mon. Wea. Rev.*, **122,** 686–702.

Waters, J. W., L. Froidevaux, W. G. Read, G. L. Manney, L. S. Elson, D. A. Flower, R. F. Jarnot, and R. S. Harwood, 1993a: Stratospheric ClO and O_3 from the Microwave Limb Sounder on the Upper Atmosphere Research Satellite. *Nature,* **362,** 597–602.

——, ——, G. L. Manney, W. G. Read, and L. S. Elson, 1993b: MLS observations of lower stratospheric ClO and O_3 in the 1992 Southern Hemisphere winter. *Geophys. Res. Lett.*, **20,** 1219–1222.

——, G. L. Manney, W. G. Read, L. Froidevaux, D. A. Flower, and R. F. Jarnot, 1995: UARS MLS observations of lower stratospheric ClO in the 1992–93 and 1993–94 Arctic winter vortices. *Geophys. Res. Lett.*, **22,** 823–826.